29, 1103 (1972).
[15]L. Ley, R. A. Pollak, S. Kowalczyk, and D. A. Shirley, Phys. Lett. A 41, 429 (1972).
[16]R. A. Pollak, S. Kowalczyk, L. Ley, and D. A. Shirley, Phys. Rev. Lett. 29, 274 (1972).

PHYSICAL REVIEW B VOLUME 7, NUMBER 12 15 JUNE 1973

Compositional Trends in the Optical Properties of Amorphous Lone-Pair Semiconductors*†

Marc Kastner‡§
Department of Physics, The University of Chicago, Chicago, Illinois 60637
(Received 13 December 1972)

The pressure and temperature dependence of the refractive index and absorption edge have been measured for a group of amorphous semiconductors with average coordination number between two and four, all containing group-VI elements in twofold coordination (lone-pair semiconductors). Clear compositional trends are observed in the pressure dependence of the optical properties when these measurements are compared with the values for tetrahedral semiconductors. The chemical-bond approach is extended by the introduction of a new material parameter, the average bond-free solid angle (BFSA), in order to explain the large positive pressure coefficient of refractive index $(\partial n/\partial P)_T$ observed for chalcogenide-rich materials and the small negative values observed for tetrahedral semiconductors. BFSA is the solid angle, associated with each atom, which is free of bond charge. When BFSA is large, atoms can move closer together under stress without compressing bonds. In this case local-field corrections cause positive $(\partial n/\partial P)_T$. When BFSA is small, local-field corrections are smaller because the charge density is more uniformly distributed. Strain results in bond compression which gives negative $(\partial n/\partial P)_T$. It is found that BFSA can also explain compositional trends in the pressure coefficient of the absorption edge as well as trends in apparently unrelated material properties such as melting temperature.

I. INTRODUCTION

The chemical-bond approach to the origin of electronic states in solids has long been ignored by solid-state physicists since it cannot predict details of the electronic wave functions as can band theory. Chemical-bond arguments are capable, however, of predicting trends within classes of materials and therefore suggesting new materials with interesting properties. The chemical-bond approach is especially valuable in dealing with the properties of amorphous covalently bonded solids. Band theory is inadequate for these materials because they do not possess long-range order. On the other hand, their short-range order can be predicted or described by simple chemical-bond arguments.

Recently Phillips[1] has put the chemical-bond approach to solids on a firmer physical basis. He pointed out that chemical-bond arguments can be useful in describing properties which are determined by some average over all the valence electrons. In certain cases the low-frequency limit of the real part of the electronic dielectric constant is determined predominantly by the polarizability of the valence electrons. Phillips has used the dielectric constant to predict and understand trends within the class of A^NB^{8-N} crystals. He uses the dielectric constant to obtain a spectroscopic bond energy which is then separated into ionic and homopolar parts. A critical assumption in this analysis is that the homopolar part of the bond energy depends only on bond length a and goes as $a^{-2.5}$. Van Vechten[2] showed that this explains the negative pressure coefficient of refractive index $(\partial n/\partial P)_T$ observed for A^NB^{8-N} tetrahedrally coordinated crystals.

It has been found,[3] however, that amorphous semiconductors containing large concentrations of group-VI elements in twofold coordination have positive $(\partial n/\partial P)_T$. It was pointed out that although the chemical bonding in these materials is very different from that in tetrahedral semiconductors [different enough, in fact, that they form a distinct class of materials—lone-pair (LP) semiconductors], nonetheless this difference in bonding cannot explain the different $(\partial n/\partial P)_T$. By invoking the Lorenz-Lorentz local-field correction, we can explain the positive values of $(\partial n/\partial P)_T$ observed for materials very rich in group-VI elements. However, in order to understand the continuous change from positive to negative $(\partial n/\partial P)_T$ as composition is varied in Se-Ge, we are forced to introduce in this work a new material parameter which is called the average bond-free solid angle (BFSA). In Sec. III BFSA is described, and its relation to the different chemical bonding in LP and tetrahedral materials is discussed.

The transitions in the values of $(\partial n/\partial P)_T$ and the pressure coefficient of the absorption edge have not

been previously observed because there has been no survey of the pressure dependence of the optical properties of semiconductors ranging in composition from materials with low coordination number like Se to tetrahedral materials like Ge. Connell and Paul[4] measured the pressure coefficient of the refractive index and absorption edge of some tetrahedral amorphous semiconductors. Several authors[5–8] have studied the pressure dependence of one optical property of a single material. It is only by studying a number of different materials, however, that compositional trends can be observed.

The pressure and temperature dependence of the refractive index and the absorption edge has been studied for six amorphous LP semiconductors: As_2S_3, As_2Se_2, GeSeTe, $GeSe_2$, GeSe, and an alloy glass $Ge_{16}As_{35}Te_{28}S_{21}$ (henceforth called alloy A). In Secs. IV and V we explore the compositional trends observed in the pressure dependence of the refractive index and in some other material parameters for these and related materials. In the remaining sections we examine the pressure dependence of the absorption edge and the temperature dependence of the refractive index and absorption edge to see whether compositional trends in these parameters can be explained by chemical-bond arguments.

II. EXPERIMENTAL DETAILS

The absorption edge and wavelength of the interference fringes well below the absorption edge were measured in an Aminco optical transmission cell with sapphire windows using He as the pressure medium. The sample covered half of the cell windows, and the pressure cell was mounted on a milling table so that the sample could be moved reproducibly in and out of the light beam. In this way the transmission of the cell windows with and without the sample could be measured at any pressure in a time short enough that the intensity of the light source and the sensitivity of the detector did not change. A Perkin Elmer Model 98 monochromator and a PbS detector were used.

The maximum pressure applied was 2 kbar, which is not very high. Higher pressures make measurements more precise, but strain becomes nonlinear at higher pressures. The temperature of the pressure vessel could be varied between − 80 and 100 °C. Thin samples were prepared by radio-frequency sputtering onto plastic-coated glass substrates. The plastic was then dissolved leaving self-supporting thin films 3–15 μm thick.

For As_2S_3 the technique of Schneider and Vedam[6] was employed. The sample was plane parallel and 1 mm thick. A broadened beam from a He-Ne laser operating at 3.391 μm was focused onto the sample, creating a circular fringe pattern in reflection at near-normal incidence. When the pressure or temperature is changed, the fringes move toward or away from the center of the circular pattern. The direction of this shift gives the sign of $(\partial n/\partial P)_T$ or $(\partial n/\partial T)_P$, and the number of fringes moving past a given position gives the magnitude. The fringe shift was measured by locating a InSb photodiode (smaller than a single fringe) in the region of the fringe pattern and observing the oscillations of the output of the photodiode as the fringes move past it. The technique of Schneider and Vedam improves the precision of the measurement but can be used only with bulk samples that have plane parallel surfaces. For the thin-film samples the shift with pressure or temperature of the *wavelength* of the interference fringes was measured in transmission. The refractive index was always measured in a spectral region sufficiently below the absorption edge that n is independent of photon energy.

A change of pressure or temperature induces a shift of the interference fringes as well as a change of transmission in the spectral region of the absorption edge. Since both the refractive index n and the sample thickness l change with pressure P or temperature T the shift of the interference fringes gives the change of optical path length nl which is related to the change of n as

$$\frac{1}{nl}\left(\frac{\partial(nl)}{\partial P}\right)_T = \frac{1}{n}\left(\frac{\partial n}{\partial P}\right)_T - \frac{K}{3} \tag{1}$$

for pressure or

$$\frac{1}{nl}\left(\frac{\partial(nl)}{\partial T}\right)_P = \frac{1}{n}\left(\frac{\partial n}{\partial T}\right)_P + \frac{\beta}{3} \tag{2}$$

for temperature, where $K = -(1/V)(\partial V/\partial P)$ and $\beta = (1/V)(\partial V/\partial T)_P$. The measured values of $(1/nl) \times [\partial(nl)/\partial T]_P$ and $(1/nl)[\partial(nl)/\partial P]_T$ are listed in Table I.

The absorption coefficient α was measured at values of transmission small enough that multiple reflection could be neglected. For As_2S_3 and alloy A absorption-edge measurements were also made on thick (1–2 mm) samples. As discussed in detail below, the change in transmission is interpreted as a

TABLE I. Pressure and temperature coefficients of the optical path length (nl) and absorption edge (E_0) of amorphous materials.

Material	$\frac{1}{nl}\left(\frac{\partial(nl)}{\partial P}\right)_T$ (10^{-6} bar^{-1})	$\frac{1}{nl}\left(\frac{\partial(nl)}{\partial T}\right)_P$ (10^{-4} K^{-1})	$\left(\frac{\partial E_0}{\partial P}\right)_T$ (10^{-5} eV bar^{-1})	$\left(\frac{\partial E_0}{\partial T}\right)_P$ (10^{-4} eV K^{-1})
As_2S_3	3.6±0.2	0.17±0.01	−1±0.2[b]	−3±2
As_2Se_3	4.9±0.6	0.4±0.2	−1.3±0.1	−7.0±0.4
Alloy A	5.5±1	0.4±0.4	−1.5±0.1[c]	−5±1
GeSeTe	2.6±0.3	0.4±0.1	−1.0±0.1	−5.9±0.8
$GeSe_2$	<0.5	<0.2	−0.9±0.1	−9.5±0.4
GeSe	<1	1.8±0.4	<0.3	−6.9±0.9

[a] E_0 was measured at absorption coefficient $\alpha = 10^3$ cm^{-1}.
[b] Measured at $\alpha = 10$ cm^{-1} and 10^3 cm^{-1}.
[c] Measured at $\alpha = 1$ cm^{-1} and 10^3 cm^{-1}.

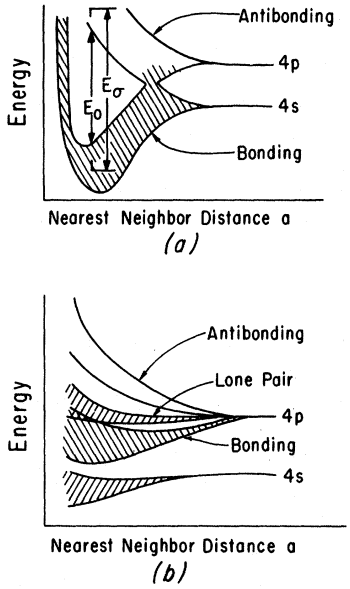

FIG. 1. Sketch of energy bands versus bond length a (nearest-neighbor distance) (a) for Ge and (b) for Se.

shift of the absorption-edge energy E_0. The measured values of $(\partial E_0/\partial P)_T$ and $(\partial E_0/\partial T)_P$ are given in Table I.

Several trends are clear in Table I. The values of $(1/nl)\,[\partial(nl)/\partial P]_T$ are positive for the chalcogenide-rich materials. This is surprising because tetrahedral semiconductors have negative $(1/nl)[\partial(nl)/\partial P]_T$. The values of $(\partial E_0/\partial P)_T$ are negative for the materials listed in Table I. This is also surprising since amorphous tetrahedral materials all have positive $(\partial E_0/\partial P)_T$. Furthermore, the magnitudes of $(\partial E_0/\partial P)_T$ and $(1/nl)\,[\partial(nl)/\partial P]_T$ are smaller for the Ge-rich materials than for the chalcogenide-rich materials. It appears that a continuous transition takes place in the pressure derivatives of the refractive index and the absorption edge as one varies composition between the chalcogenide materials and the tetrahedral semiconductors.

III. CHEMICAL BONDING AND CLOSED-SHELL INTERATIONS

To discuss the experimental data in greater detail, the chemical-bond approach developed by Mooser and Pearson[9] will be helpful. The basic assumption made is that the electronic states of the solid are a broadened superposition of molecular states arising from the constituent bonds. With this assumption one can describe qualitatively how atomic orbitals form bonds which are broadened into bands in the solid. One can plot the energy of electronic states as a function of nearest-neighbor distance a, as sketched qualitatively in Fig. 1 for Ge and Se. We note that the valence band in Ge is primarily a bonding band and the conduction band is primarily an antibonding band. In Se the valence band is a filled nonbonding or lone-pair (LP) band. The latter has been discussed previously[10] and it was pointed out that in any amorphous semiconductor containing group-VI elements in twofold coordination, the LP band is the valence band.

A unversal feature of Fig. 1 is that bond energies (bonding-antibounding energy separation) get smaller as a increases. Also universal is the fact that the bands broaden as a decreases.

Figure 1 describes the covalent bonding in semiconductors. This may be sufficient for a qualitative understanding of the pressure dependence of the optical properties of tetrahedral network structures, but this is not the case for chalcogenide glasses. Ge, for example, is tetrahedrally coordinated. When stress is applied, atoms can move closer together only by compressing covalent bonds. The effects of pressure are then described by Fig. 1(a). Se, on the other hand, is twofold coordinated. It forms rings (monoclinic) or chains (trigonal). The bond angle in both cases is about 100°.

In Figs. 2(a) and 2(b) are sketched the coordination tetrahedron of Ge and the charge-density distribution in one of the four sp^3 bonding orbitals. One can see that the four bonds virtually fill the tetra-

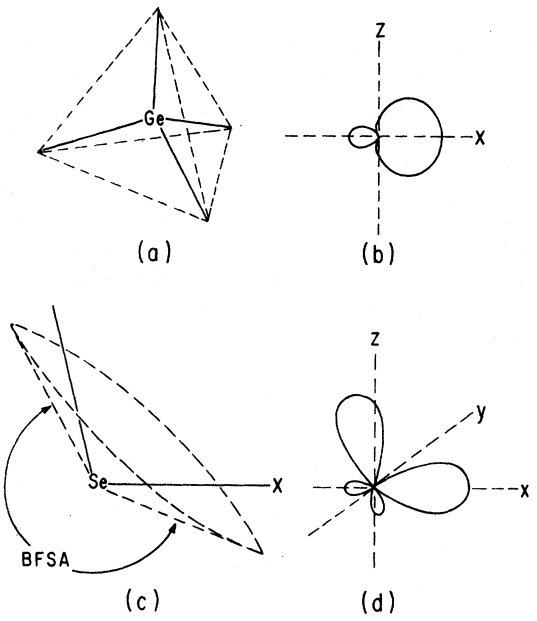

FIG. 2. (a) Coordination tetrahedron of Ge. Solid lines represent bond directions. (b) Charge-density distribution in one of the four sp^3 hybridized orbitals of Ge. (c) Twofold coordination of Se. Solid lines represent bond directions. Cone contains most of the bond charge so the solid angle outside the cone is the BFSA. (d) Charge-density distribution in the two (predominantly p) bonds of Se.

hedron so there is very little solid angle that is free of bond charge. Figures 2(c) and 2(d) show the twofold coordination of Se and the charge-density distribution for the two bonds. The lone-pair charge density will be distributed primarily where there is no bond charge: in the $(-x, -z, \pm y)$ quadrants. If we draw a cone as in Fig. 2(c) with its vertex at the Se atom containing most of the bond charge (but not the lone pair), it is clear that there is a large solid angle (4π minus the solid angle of cone) that is free of bond charge. This is what is called the bond-free solid angle (BFSA). Alternatively this might be called approach solid angle, i.e., that solid angle in which a second atom can approach the first atom with compressing covalent bonds. Of course, the magnitude of the approach angle depends on the size and coordination of both atoms. In the following the term BFSA is used but the approach-angle concept should be kept in mind.

There is therefore a large solid angle associated with each Se atom in solid Se in which there are no covalent bonds. In these directions the overlap of the charge density of a Se atom on one chain or ring with the atoms on an adjacent chain or ring is relatively small. Other atoms can approach a Se atom from these directions without compressing bonds. Only closed-shell interactions will be important when atoms approach each other in this way. A similar mechanism is possible for group-V elements that are threefold coordinated, but the bond-free solid angle is smaller.

Closed-shell interactions have been analyzed in great detail for molecular liquids or solids. When orbital overlap is small, one can make a multipole expansion of the potential perturbing a given molecule in the presence of its neighbors.[11] Perturbation theory then gives the resulting energy shifts of the molecular levels. If the molecules have no charge and no dipole moment, the first term in the perturbation expansion is the dispersion energy

$$U_d = -\sum_{ij} \frac{|H_{ij}|^2}{E_i - E_j} \quad , \tag{3}$$

where $|H_{ij}|^2$ is the induced dipole-induced dipole interaction which varies like $1/R^6$. The sum is taken over all filled states j and empty states i of the isolated molecule. The second term is the exchange repulsion term which according to Mulliken[12] can be approximated by

$$U_{eR} \propto \frac{S^2}{R}, \tag{4}$$

where S is the orbital overlap and R is the intermolecular separation. This term, together with the dispersion energy, gives rise to what are commonly called Van der Waals forces. These are the closed-shell interactions which will be most important in the materials discussed here. As the distance between closed shells decreases, the bands of states associated with electrons in these closed shells broaden because of the increased overlap between neighboring closed shells.

The effects of closed-shell interactions are dramatically illustrated in Fig. 3, which shows the band structures of trigonal Se and Te calculated by Treusch and Sandrock.[13] The large dispersion at K in the Brillouin zone is probably due to dispersion forces between chains. Note that the bands are much flatter in other regions of the zone. This may, however, be a residue of the free-electron bands which have a large separation at K, whereas at H the free-electron valence and conduction bands are degenerate. The broadening of the bands associated with overlap of electrons in closed shells on different chains is seen in Fig. 3 as an increased splitting of each of the three triplets near K, which is the direction of greatest overlap.

In general the force constants associated with closed-shell interactions are smaller than those associated with covalent bonds. If the BFSA is large, pressure should therefore affect closed-shell interactions more than covalent bonds. In

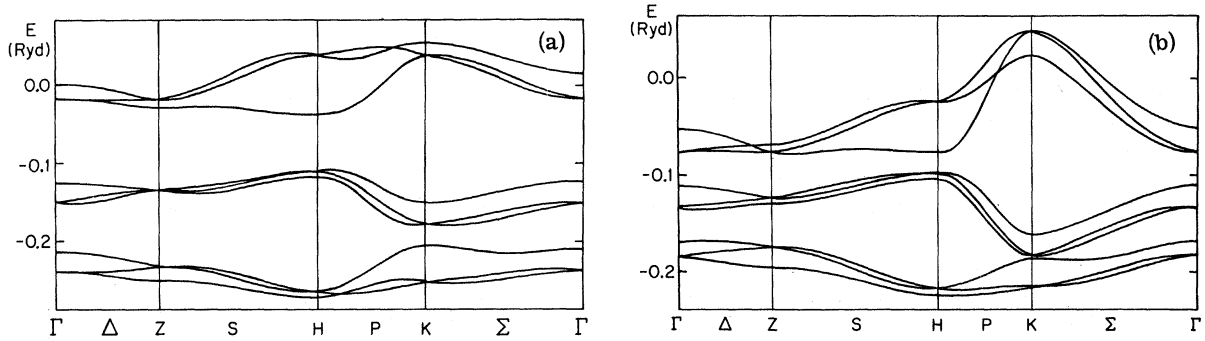

FIG. 3. Energy band structure of (a) Se and (b) Te after Treusch and Sandrock (Ref. 13).

materials with cross-linked network structures like $GeSe_2$ or SiO_2, atoms can move closer together only by bending or stretching bonds, even though some atoms have very large BFSA. Bond-bending force constants are generally smaller than stretching force constants[14] so we expect bond bending to be important for these materials.

In Sec. IV the pressure dependence of the refractive index for a group of amorphous semiconductors is examined. The results indicate that local-field corrections are important for materials with large BFSA.

IV. PRESSURE DEPENDENCE OF REFRACTIVE INDEX AND LOCAL-FIELD CORRECTIONS

The pressure dependence of the refractive index $(\partial n/\partial P)_T$ of several amorphous chalcogenide semiconductors was discussed in detail in a previous paper.[3] In Table II values of n, $(1/nl)[\partial(nl)/\partial P]_T$, K, and $(1/n)(\partial n/\partial P)_T$ are listed for the six materials mentioned above and for several other materials for comparison. $(\partial n/\partial P)_T$ is positive for the chalcogenide amorphous semiconductors and negative for the tetrahedral materials. In Ref. 3 it was argued that if the primary effect of pressure is to decrease covalent bond length a, as in Si or GaAs, then $(\partial n/\partial P)_T$ will be negative. In this case, as pointed out by Van Vechten[2] and Phillips,[14] n measures the strength of the chemical bond (bonding-antibounding energy separation) which decreases with increasing a. On the other hand, if the BFSA is large, the primary effect of pressure is to force closed shells closer together without changing covalent bond lengths. In this case local-field corrections result in positive $(\partial n/\partial P)_T$.

Wiser[15] calculated the local-field correction to

TABLE II. Data and calculated parameters for amorphous (a-) and crystalline (c-) materials. K is compressibility, n is refractive index, l is sample thickness, and η is defined in Eq. (11).

Material	K (10^{-6} bar^{-1})	$\frac{1}{nl}\left(\frac{\partial(nl)}{\partial P}\right)_T$ (10^{-6} bar^{-1})	$\frac{1}{n}\left(\frac{\partial n}{\partial P}\right)_T$ (10^{-6} bar^{-1})	n	η	$-\frac{1}{2}(n^2+2)$	Reference[a]
a-alloy A	7.6[b]	5.5±1	8.0±1.5	3.1±0.1	−3.5±0.4	−5.8±0.4	P
a-As_2S_3	9.3±0.4[c]	3.6±0.2	6.8±0.4	2.41[d]	−2.5±0.1	−3.9	P
a-As_2Se_3	6.4[e]	4.9±0.6	7.0±0.6	2.6	−3.8±0.3	−4.4	P
a-GeSeTe		2.6±0.5		2.2			P
a-$GeSe_2$		0±0.5		2.2			P
a-GeSe		0±1		2.6			P
a-Se	10.0[f]	7.7	11.0	2.5[g]	−3.9	−4.1	h
c-SiO_2	2.6	−0.19	0.667	1.54	−1.32	−2.18	i
a-SiO_2	2.69	−0.26	0.631	1.46	−1.33	−2.06	j
c-Al_2O_3	0.40	−0.19	−0.06	1.77	0.66	−2.56	k
c-CaF_2	1.22	−0.237	0.170	1.43	−0.81	−2.06	l
c-BaF_2	1.96	−0.219	0.434	1.47	−1.23	−2.17	l
c-PbF_2	1.64	−0.107	0.440	1.77	−1.18	−2.56	l
Diamond	0.173		−0.053	2.42	1.1	−3.92	m
a-Si			−0.05				n
c-Si	1.02	−0.6	−0.3	3.4	1.0	−6.8	n
a-Ge			−0.8				n
c-Ge	1.33	−1.4	−1.0	4.0	2.3	−9.0	n
a-GaP			−0.25				n
c-GaP	1.13	−0.7	−0.3	3	0.9	−5.5	n
a-GaAs			−0.7				n
c-GaAs	1.34	−1.1	−0.7	3.4	1.8	−6.8	n

[a]Reference gives all data except where noted. P denotes present work.

[b]From 0.1% measurements of longitudinal and transverse sound velocity, D. E. Bowen (private communication).

[c]Obtained from Young's modulus and shear modulus furnished by Servo Corporation of America.

[d]Servo Corporation of America.

[e]A. P. Chernov, S. A. Dembovsky, and S. F. Chistov, SSSR Neorgan. Mater. 4, 1663 (1968).

[f]K. Vedam, D. L. Miller, and R. Roy, J. Appl. Phys. 37, 3432 (1966).

[g]W. F. Koehler, F. K. Odencrantz, and W. C. White, J. Opt. Soc. Am. 49, 109 (1959).

[h]Reference 6.

[i]T. A. Davis and K. Vedam, J. Opt. Soc. Am. 57, 1140 (1967).

[j]K. Vedam, E. D. D. Schmidt, and R. Roy, J. Am. Ceram. Soc. 49, 531 (1966).

[k]T. A. Davis and K. Vedam, J. Appl. Phys. 38, 4555 (1967).

[l]E. D. D. Schmidt and K. Vedam, J. Phys. Chem. Solids 27, 1563 (1966).

[m]D. F. Gibbs and G. J. Hill, Phil. Mag. 9, 367 (1964)

[n]Reference 4.

the dielectric constant in the weak and tight-binding limits. He defines a generalized local field as that quantity which determines the polarization per electron. It is obtained by averaging the microscopic field $\vec{E}(\vec{r})$ over the region occupied by the electron, the contribution to the average being greater from those parts of the unit cell where the electron is more easily polarized:

$$\vec{E}_{\rm loc}(\vec{r}) = \frac{\int d\vec{r} \int d\vec{r}'\ \alpha_p(\vec{r},\vec{r}')\vec{E}(\vec{r}')}{\int d\vec{r} \int d\vec{r}'\alpha_p(\vec{r},\vec{r}')} \quad . \tag{5}$$

The microscopic polarizability $\alpha_p(\vec{r},\vec{r}')$ is related to the polarization $\vec{P}(\vec{r})$ by

$$\vec{P}(\vec{r}) = N \int d\vec{r}'\ \alpha_p(\vec{r},\vec{r}')\vec{E}(\vec{r}') \ , \tag{6}$$

where N is the atomic density.

When the charge distribution is spatially uniform the local field equals the macroscopic field, which is the unweighted spatial average of the microscopic field. This leads to the Drude relation for the dielectric constant ϵ:

$$\epsilon - 1 = 4\pi N\alpha_p \ , \tag{7}$$

where α_p is the polarizability per atom. However, in the tight-binding limit, Eq. (6) reduces to

$$\vec{P} = N\alpha_p \vec{E}_{\rm loc} \ , \tag{8}$$

with

$$\alpha_p = \int_\Omega \alpha_p(\vec{r},\vec{r}')\, d\vec{r}' \quad .$$

Here Ω is the volume of integration associated with a single bond or atom. If Ω for a given atom or bond overlaps the volume of integration for adjacent atoms or bonds, relation (8) is not expected to be valid. In the tight-binding limit the local field is quite different from the macroscopic field. The local field $E_{\rm loc}$ is given by

$$\vec{E}_{\rm loc} = \vec{E} + 4\pi\gamma\vec{P} \ , \tag{9}$$

where $\gamma = \frac{1}{3}$ for cubic or isotropic systems. This results in the Lorenz-Lorentz (LL) relation for the dielectric constant:

$$\frac{\epsilon - 1}{\epsilon + 2} = \frac{4\pi}{3} N\alpha_p \ . \tag{10}$$

It is not easy to test experimentally whether the local-field correction is negligible in systems like Ge or Si. Van Vechten[2] assumes that this is the case and uses the Drude relation. It is easy, however, to test whether the LL relation is applicable, for in that case α_p computed from Eq. (10) is independent of density.

Summarizing Wiser's results: If the charge density that determines ϵ is distributed uniformly in space, then the Drude relation is applicable. When the charge density is localized, however, local-field corrections are large and the LL relation properly describes the dielectric constant.

For predicting the experimental values of $(\partial n/\partial P)_T$ either with the Drude or LL relation, it is convenient to examine the quantity

$$\eta = \frac{l}{n}\left(\frac{\partial n}{\partial l}\right)_T \frac{n^2}{n^2-1} = \frac{l}{2\epsilon}\left(\frac{\partial \epsilon}{\partial l}\right)_T \frac{\epsilon}{\epsilon - 1} \quad . \tag{11}$$

For tetrahedral semiconductors Van Vechten assumes local-field corrections are negligible and uses a special form of the Drude relation, a modified Penn–Phillips relation, for the dielectric constant:

$$\epsilon - 1 = (\hbar\omega_p/E_\sigma)^2 \ . \tag{12}$$

From this one predicts

$$\eta = -\frac{3}{2} - \frac{l}{E_\sigma}\frac{dE_\sigma}{dl} \quad . \tag{13}$$

Here ω_p is the plasma frequency arising from the valence electron density and E_σ is a modified Penn-Phillips gap. The $-\frac{3}{2}$ term arises from the volume dependence of $\omega_p \sim l^{-3/2}$. In materials with small bond-free solid angle like Si or GaP, the measured strain dl/l equals the fractional change in bond length da/a. In this case we expect $\eta > 0$ since dE_σ/da is negative, as can be seen in Fig. 1. For group-IV elements, for example, $(a/E_\sigma)\, dE_\sigma/da = -2.5$ and $\eta = 1.0$. The experimental values for diamond and Si are in agreement with this prediction. Van Vechten explains that Ge or GaAs should have $\eta > 1$ because of the contribution of d electrons to n.

To test whether the LL relation applies to a given material, one must test whether α_p in Eq. (10) is independent of density. When this is the case, the prediction for η from Eq. (10) is

$$\eta = -\tfrac{1}{2}(\epsilon + 2). \tag{14}$$

Table II shows that this prediction is within a few percent of the experimental value for Se. For materials containing group-IV and group-V elements, the agreement is not as good. Of course, for the tetrahedral materials Eq. (14) fails completely.

There is further evidence that the polarizability calculated from Eq. (10) is independent of volume for Se. When amorphous Se crystallizes the density changes by about 10%, but if the chemical bonding does not change much, then α_p should not change. Calculating α_p from the measured density and refractive index for the amorphous and crystalline phases, we find

$$\alpha_p = (4.79 \pm 0.36) \times 10^{-22}\ \text{cm}^3 \quad \text{(crystal)}$$

$$= (4.54 \pm 0.02) \times 10^{-22}\ \text{cm}^3 \quad \text{(amorphous)} \ .$$

From the success of the LL relation in predicting the refractive index of Se for the amorphous and crystalline phase and the pressure dependence of the refractive index, it appears that for this material different methods of varying the density will

give the same strain dependence of n. For cross-linked glasses, however, this is not the case. Spinner and Waxler[16] found considerable difference between the effects of annealing and compression on various silicate glasses. They found that for a given increase of density on annealing the increase in index is greater than for the same increase of density on compression. One concludes that annealing not only causes a change in density but a change and rearrangement of chemical bonds.

There is one experiment that casts some doubt on our application of Eq. (10) to Se. This is the piezobirefringence (B_p):

$$B_p = \frac{\epsilon_{\parallel} - \epsilon_{\perp}}{G} , \tag{15}$$

where $\epsilon_{\parallel}$ and $\epsilon_{\perp}$ are refractive indices for light polarized parallel and perpendicular, respectively, to the direction of uniaxial stress. G is the magnitude of the stress.

We assume α_p is not affected by stress. If the LL relation gives α_p independent of density for hydrostatic pressure, we expect α_p to be independent of density for uniaxial stress as well. Eq. (9) gives

$$\epsilon = \frac{1 + 4\pi N\alpha_p(1 - \gamma)}{1 - 4\pi N\alpha_p\gamma} . \tag{16}$$

If the hydrostatic pressure measurement agrees with Eq. (14) as it does for Se, then $\gamma = \frac{1}{3}$. When uniaxial stress is applied γ is no longer isotropic. Consider a cube within the unstrained material with edges along the x, y, and z directions. Tensional stress along the z axis will change this cube into a rectangle of square cross section. The ratio of the lengths of the edges will then be $x : y : z :: 1 : 1 : 1 + \Delta$. For a uniaxial stress G, $\Delta = G(1 + \sigma)/Y$. Here σ is Poisson's ratio and Y is Young's modulus. If z is the direction of stress, Mueller[17] has shown that

$$\gamma_z = \gamma - \Delta, \quad \gamma_x = \gamma_y = \gamma + \tfrac{1}{2}\Delta . \tag{17}$$

Mueller's calculation was actually for a cubic solid but for small Δ the results are expected to be identical for an amorphous solid. Differentiating (16) and using (17), we find

$$B_p = -\tfrac{3}{2}(\epsilon - 1)^2(1 + \sigma)/Y. \tag{18}$$

For Se this yields $B_p = -5.5 \times 10^{-4}$ bar^{-1}, whereas Yu and Cardona[18] measured $B_p = -1 \times 10^{-5}$ bar^{-1}. Yu and Cardona interpreted their results with a Drude relation. Then B_p arises predominantly from bond stretching. They must then assume $dE_g/da > 0$ to obtain the observed sign of B_p. This is inconsistent with our understanding of the covalent bond as sketched in Fig. 1. Although Eq. (18) predicts a value of B_p much larger in magnitude than is observed, the sign is correct. The piezobirefringence is the only measurement that casts doubt on the application of Eq. (10) to Se. In the following discussion it is assumed that the Lorenz-Lorentz relation properly describes the local field correction in Se. It is important to note, however, that the peizobirefringence cannot be described by such a simple relation, and therefore that this measurement may be more sensitive to the character of the local field (particularly its anisotropy) than the hydrostatic pressure measurement.

According to Wiser, the localization of the valence charge density determines the magnitude of the local-field correction. Only in the tight-binding limit does one expect α_p to be independent of volume. However, Se is not generally considered to be a tight-binding solid. Certainly if one tried to calculate the polarizability from Eq. (8) for a Se chain the volume of integration for a given covalent bond would overlap that of adjacent bonds, and by that criterion the LL relation should not be valid. However, the same argument can be made for large organic molecules and yet liquid and solid hydrocarbons also have α_p independent of volume.[19]

In trigonal Se, although the charge density is not localized in the direction along the chains, it is localized in the directions between chains. Charge-density overlap is large where atoms are chemically bonded but not in the bond-free solid angle. For such cases the local-field correction itself, not just the polarizability tensor, is anisotropic.

One still might expect the local-field correction for Se to be smaller than that given by the LL relation. Se has a BFSA smaller than 4π, and only for that case does one expect the LL relation to be exact. It might be that the reason for the unusually good agreement in the case of Se is the lone-pair valence band. Most of the polarizability of Se arises from lone pair to antibonding transitions.[3] Lone pairs are probably more localized than bonding electrons because of the small nearest-neighbor overlap. If, therefore, the valence electron density is localized, the LL relation is the proper description of the dielectric constant.

Consider now adding Ge to amorphous Se. As the Ge concentration is increased, a cross-linked network is formed. As in the case of pure Se, the BFSA associated with each Se atom is large, and the local field felt by the charge density associated with a given Se atom is affected by nonoverlapping charge densities in these bond-free directions. However, because of the cross-linked network, these nonoverlapping charge densities cannot approach each other without compressing or bending bonds. The fraction of atoms with large BFSA is decreased in proportion to the concentration of Ge atoms. Because of the resulting increase in charge-density overlap, local-field corrections are reduced. Furthermore, as the concentration of Ge increases, the number of LP electrons per atom decreases. If the bonding electrons are less lo-

calized than the LP electrons, then the local-field correction will become smaller as the bonding band contributes a larger fraction of the polarizability. There are therefore three coupled effects which reduce the pressure coefficient of the refractive index: (i) As the average bond-free solid angle decreases, local-field corrections are reduced, (ii) strain increasingly involves bond bending and bond compression; and (iii) the bonding band contributes a larger fraction of the total polarizability with a resulting decrease in the local-field correction. These effects probably are the cause of the transition from positive to negative $(\partial n/\partial P)_T$ in going from chalcogenide-rich to tetrahedral amorphous semiconductors.

In order to make approximate predictions for cases intermediate between the weak- and tight-binding limits, several authors[20] assume the full LL relation and describe any deviations from the prediction of Eq. (10) as a change in α_p with pressure. They replace Eq. (14) by

$$\eta = -\tfrac{1}{2}(\epsilon+2)(1-\Lambda_0) \tag{19}$$

with $\Lambda_0 = (V/\alpha_p)(\partial \alpha_p/\partial V)_T$. This incorporates the intuitive notion that α_p will be pressure dependent if strain requires bond compression but assumes that the LL relation correctly describes the local-field correction for all materials. Van Vechten uses the Drude relation (no local-field correction) and assumes that the pressure dependence of different materials is given by different $(\partial \alpha_p/\partial V)_T$ or dE_σ/da. He assumes that there is no local-field correction for any $A^N B^{8-N}$ material—even alkali halides for which the charge density is quite localized. Finally, there is the approach of Mott and Gurney,[21] who assume that ϵ can be described by Eq. (16), where γ gives the strength of the local-field correction. For $\gamma = \frac{1}{3}$ one obtains the LL relation, and for $\gamma = 0$ one obtains the Drude relation. This approach assumes α_p is independent of pressure, which is a very bad approximation when strain requires bond compression. Clearly there is no simple relation that adequately describes the dielectric constant of materials which have intermediate BFSA or intermediate charge localization. Most chalcogenide glasses fall into this category, as can be seen from the values of η or $(1/nl)[\partial(nl)/\partial P]_T$ given in Table II.

When it is observed that the dielectric constant obeys Eq. (10) with α_p independent of volume, we conclude that the BFSA is large. Hilton[22] used Eq. (10) to predict ϵ for more than 20 chalcogenide glasses with an average error of 4%. He assumed $\alpha_p = \sum_i x_i \alpha_i$, where x_i is the concentration of the ith element and α_i is some average atomic polarizability calculated from the covalent radius ($\alpha_i \sim r_i^3$, where r_i is the covalent radius). From these results we can conclude that the covalent bonding of a given element is the same in all the materials he studied. This is not too surprising because the elements in Hilton's glasses have similar electronegativity. Furthermore, to the extent that the density changes from one material to another, additivity requires large BFSA because α_p is independent of density. In the materials studied by Hilton, however, the atomic density is almost constant, so the additivity of α_p does not in this case prove that BFSA is large. The results of Hilton are reproduced in Table III.

The pressure dependence of the refractive index is sensitive to closed-shell interactions because the force constants associated with these interactions are small and because the small charge-density overlap results in large local-field corrections. It appears that within the group of the six materials studied, a continuous transition takes place in the pressure dependence of the refractive index because the bond-free solid angle is large for chalcogenide-rich materials but small for tetrahedral materials. In Sec. V some other material parameters which may help to describe this transition are examined.

TABLE III. Molar refraction $(\frac{4}{3}\pi\,\alpha_p)$ determined from Eq. (10) after Hilton (Ref. 22).

Composition	Measured	Calculated	Error (%)
$P_{20}S_{80}$	7.36	8.49	+15.4
$Ge_{30}P_{10}S_{60}$	8.26	9.23	+11.7
Ge_2S_3	8.90	9.30	+6.5
As_2S_3	9.44	9.42	−0.2
Se	11.55	11.51	−0.4
$P_{10}Se_{90}$	11.17	11.44	+2.4
$P_{20}Se_{80}$	11.35	11.35	0
$As_{10}Se_{90}$	11.85	11.52	−2.9
$As_{20}Se_{80}$	11.55	11.54	−0.1
$Si_{10}Se_{90}$	11.65	11.31	−2.9
$Ge_{16}As_{47.3}Se_{36.7}$	11.33	11.56	+2.0
$Ge_{15}As_{45}Se_{40}$	11.45	11.54	−0.3
$Ge_{15}P_{15}Se_{70}$	10.70	11.36	+6.2
$Ge_{10}Se_{90}$	11.23	11.49	+2.3
$Si_{25}As_{25}Te_{50}$	13.42	14.55	+8.4
$Si_{20}P_{10}Te_{70}$	16.05	15.96	+0.4
$Si_{15}P_5Te_{80}$	16.55	16.76	+1.3
$Si_{30}As_{20}Te_{50}$	13.70	14.43	+5.3
$Si_{30}As_{30}Te_{40}$	12.95	13.74	+6.1
$Si_{20}As_{30}Te_{50}$	13.90	14.66	+5.5
$Ge_{10}As_{40}Te_{50}$	14.07	15.09	−7.3
$Ge_{10}As_{20}Te_{70}$	15.95	16.47	+3.2
$Ge_{15}As_{50}Te_{35}$	13.40	14.03	+4.7
$Ge_5As_{50}Te_{45}$	14.30	14.75	+3.1
$Ge_5As_{60}Te_{35}$	13.65	14.05	+2.8
$Ge_{15}As_{10}Te_{75}$	16.25	16.77	+3.2
$Ge_{10}As_{15}Te_{75}$	16.15	16.79	+4.0

V. OTHER MATERIAL PARAMETERS SENSITIVE TO CLOSED-SHELL INTERACTIONS

Goryunova[23] has surveyed the properties of a large number of materials which form tetrahedrally bonded crystals. She uses the average number of valence electrons per atom in trying to predict what compounds will form diamond lattices. Here one includes all s and p electrons in the valence shell. Materials with large numbers of valence electrons tend to be molecular. Group-IV elements form diamond lattices. Group-V and group-VI elements are intermediate. Most liquids or solids formed by group-VII and group-VIII elements are molecular. We consider group-V and group-VI elements intermediate since they may form solids that are molecular with very large overlap or cross-linked solids with some charge localization. Orthorhombic sulfur is clearly molecular, but because of the large overlap between chains Te cannot be considered as an ideal molecular solid. Phosphorous in some phases is clearly molecular (white P is composed of P_4 molecules) but As, Sb, and Bi are definitely not molecular. Although the average number of valence electrons per atom can give clues as to what materials will be molecular, other parameters such as the average atomic number or weight appear also to be important.

The bond-free solid angle increases as the average number of valence electrons per atom $\langle n_e \rangle$ increases. Group-IV elements have small BFSA because of their fourfold coordination, but as $\langle n_e \rangle$ increases the valence and average coordination number decrease with a corresponding increase in BFSA.

For several materials the quantity

$$\zeta = \left| \frac{2\eta - (\epsilon + 2)}{\epsilon + 2} \right| , \qquad (20)$$

which is the percent error made in using the prediction of the LL relation (10) to describe η, was computed. Note that although ζ is numerically equal to Λ_0 in Eq. (19) the concept is very different. In using Eq. (19) with $\Lambda_0 = V/\alpha_p(\partial \alpha_p/\partial V)_T$ one is assuming that the LL relation properly describes the local-field correction but that α_p is volume dependent. ζ is allowed to contain both the volume dependence of α_p and the local-field volume dependence if different from that predicted by the LL relation. ζ is plotted against $\langle n_e \rangle$ in Fig. 4. It is clear that as $\langle n_e \rangle$ increases, Eq. (10) becomes a better description of η ($\zeta = 0$ for an ideal molecular solid). Ignoring the value for PbF_2 for the moment, it appears that the transition in the pressure dependence of the refractive index occurs between $\langle n_e \rangle = 4$ and $\langle n_e \rangle = 6$. It is interesting that many materials that form glasses (amorphous solids that can be quenched from the melt) have $\langle n_e \rangle$ between 5 and 6. PbF_2 does not agree with the general trend that ζ becomes small for $\langle n_e \rangle$ near 6. Furthermore, there are some $\langle n_e \rangle = 4$ materials for which measurements have been made which are not plotted in Fig. 3. Many of these agree with the trend—they have very large ζ. The alkali halides, however, which also have $\langle n_e \rangle = 4$, have ζ of 0.5–0.7. Van Vechten[2] points out that ionicity will strongly affect the volume dependence of the refractive index. The disagreement of PbF_2 with the general trend is Fig. 4 emphasizes that the concept of BFSA is sufficient to explain trends in $(\partial n/\partial P)_T$ only for predominantly covalent materials. For the $A^N B^{8-N}$ materials BFSA is small and one need only consider trends arising from ionicity differences. But for other materials both BFSA and ionicity will be important. For example, ionicity will certainly affect the ζ of CaF_2 and BaF_2 and perhaps Al_2O_3 and SiO_2 as well.

One might expect As_2S_3 and As_2Se_3 to have the same value of ζ. The difference may arise from the slightly more ionic bonding in As_2S_3. However, it must be remembered that As_2S_3 was measured as a bulk sample and As_2Se_3 was a sputtered film. Perhaps further measurements on bulk As_2Se_3 will bring the values of ζ for the two materials closer together.

In Fig. 5 are plotted energy gap E_g vs melting point T_M for several groups of solids characterized by different $\langle n_e \rangle$. The trend in Fig. 5(a) is what is expected for cross-linked covalent solids. As the chemical bond gets stronger, the melting point gets higher because bonds must break for melting to

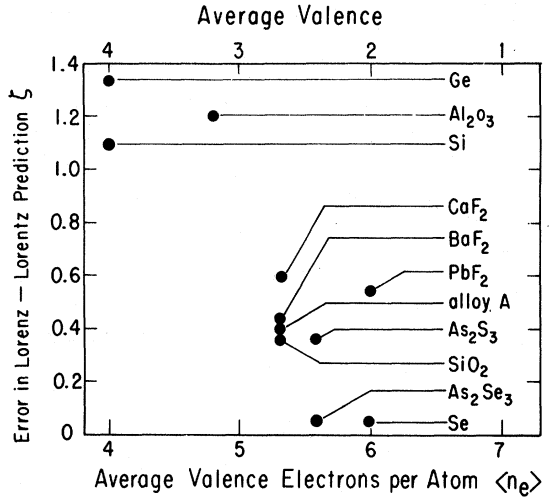

FIG. 4. Error of the Lorenz–Lorentz relation in predicting the volume dependence of refractive index (ζ) versus average number of valence electrons per atom $\langle n_e \rangle$. The valence or coordination number is given at the top of the figure. Note that group-VII elements are molecular and group-VIII are the noble gases, so for $\langle n_e \rangle = 7$ and 8, $\zeta = 0$.

take place. However, a stronger bond results in a larger band gap. Thus higher melting materials have larger band gaps. In Fig. 5(d) the opposite trend is found: for group-VI elements, the band gap decreases as melting point increases. This happens because melting in group-VI elements requires the separation of molecules but not the breaking of covalent bonds. The intermolecular binding energy has the form given in Eq. (3). The intermolecular binding is stronger if the energy separation between filled and empty states $E_i - E_j$ is *smaller*. Thus higher band-gap molecular solids have lower melting points. Once again materials with $\langle n_e \rangle = 4$ and $\langle n_e \rangle = 6$ are extremes, and compounds with $\langle n_e \rangle \sim 5$ are intermediate. Thus III_2 VI_3 compounds have T_M almost independent of E_g [see Fig. 5(c)]. Actually, one should plot a quantity which measures the bond energy vs T_M to properly examine these trends. For $\langle n_e \rangle = 4$ materials E_σ is plotted against T_M in Fig. 5(e). The trend is very similar to that in 5(a). Because of the complicated nature of the bonding in materials with $\langle n_e \rangle$ different from 4, it is not easy to determine a quantity like E_σ, which measures the bond energy for the other groups of material in Fig. 5. However, we trust that just as for $\langle n_e \rangle = 4$ materials, the trend followed by the average energy E_σ will be the same as that followed by the minimum interband energy E_g.

It should be pointed out that, for the sake of clarity, some materials for which E_g and T_M are known are not plotted in Fig. 5. Adding these points does not, however, alter the trends or increase the scatter.

However, Fig. 5 tells only part of the story. De Neufville[24] measured E_g and T_g for glasses in the $GeSe_2 - GeTe_2$ system. Using the rule of Sakka and Makenzie[25] ($T_M = \frac{3}{2} T_g$), de Neufville's results yield $\Delta E_g / \Delta T_M \sim +2 \times 10^{-3}$ eV K^{-1}. This is similar to the slope obtained from Fig. 5(a) for $\langle n_e \rangle = 4$ materials: $\Delta E_g / \Delta T_M = 3 \times 10^{-3}$ eV K^{-1}. The results of Nunoshita and Arai[26] yield $\Delta E_g / \Delta T_M = 2.6 \times 10^{-3}$ eV K^{-1} for 25 glasses in the Si-As-Te system. Thus among cross-linked glasses which have $\langle n_e \rangle$ from 5.0 to 5.7 one finds T_M *increasing* with E_g just as for $\langle n_e \rangle = 4$ materials.

These results emphasize the importance of group-IV elements in cross-linking the chalcogen polymer chains, as pointed out by de Neufville. When a glass contains a high enough concentration of group-IV elements, melting requires the breaking of covalent bonds.

The melting point vs band gap plots, like the ζ vs $\langle n_e \rangle$ plots, emphasize the importance of closed-shell interactions in materials with large bond-free solid angle. One might expect the pressure dependence of the absorption edge also to be strongly influenced by closed-shell interactions.

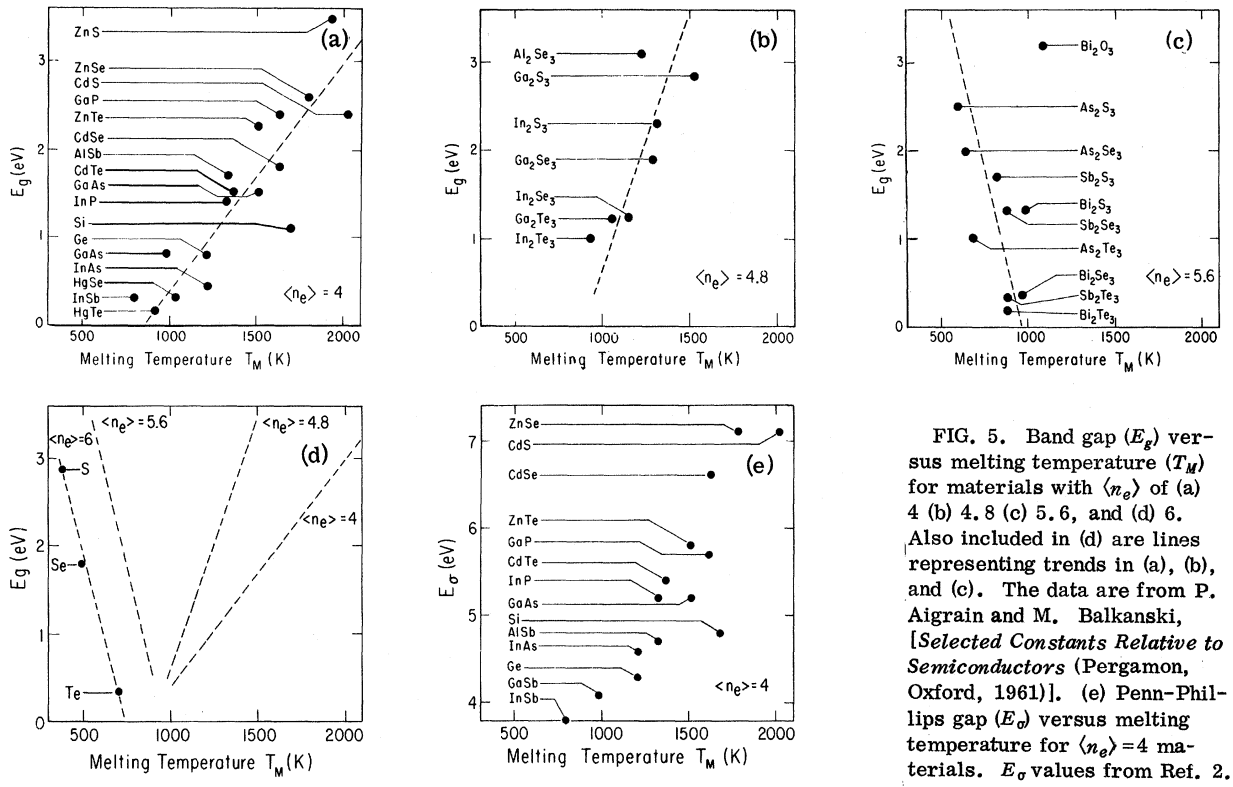

FIG. 5. Band gap (E_g) versus melting temperature (T_M) for materials with $\langle n_e \rangle$ of (a) 4 (b) 4.8 (c) 5.6, and (d) 6. Also included in (d) are lines representing trends in (a), (b), and (c). The data are from P. Aigrain and M. Balkanski, [*Selected Constants Relative to Semiconductors* (Pergamon, Oxford, 1961)]. (e) Penn-Phillips gap (E_σ) versus melting temperature for $\langle n_e \rangle = 4$ materials. E_σ values from Ref. 2.

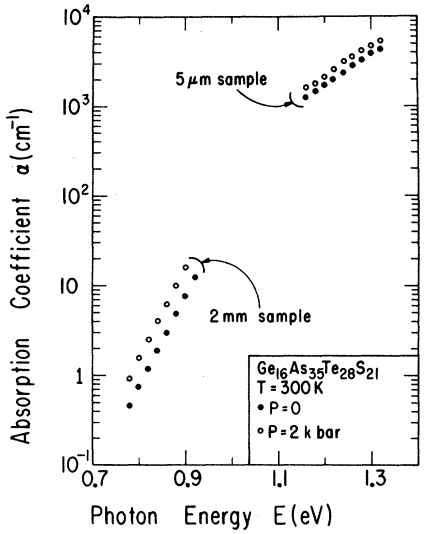

FIG. 6. Absorption coefficient (α) of alloy A versus photon energy ($\hbar\omega$) for pressures of 0 and 2 kbar at room temperature. Note that $\Delta E/\Delta P$ is independent of α.

TABLE IV. Pressure and volume coefficient of the absorption edge (E_0).

Material	$\left(\frac{\partial E_0}{\partial P}\right)_T$ (10^{-6} eV bar^{-1})	$V\left(\frac{\partial E_0}{\partial V}\right)_T$ (eV)	Reference[a]
a-As_2S_3	-10 ± 2	1.1 ± 0.2	P
a-As_2Se_3	-13 ± 1	2.0 ± 0.2	P
a-alloy A	-15 ± 1	2.0 ± 0.2	P
a-Se	-20 ± 5	2.0 ± 0.5	b
a-Si	0.25		c
c-Si	-1.5	-1.5	c
a-Ge	3.5		c
c-Ge	5.0	3.8	c
a-GaP	0.2		c
c-GaP	-1.1	-1.0	c
a-GaAs	0.7		c
c-GaAs	11.3	8.4	c

[a]P denotes present work.
[b]R. S. Caldwell and H. Y. Fan, Phys. Rev. 114, 664 (1959).
[c]Reference 4.

VI. PRESSURE DEPENDENCE OF ABSORPTION EDGE

For each of the six materials studied, the pressure dependence of the absorption edge was measured. For alloy A the pressure dependence was examined in greater detail than for most other materials. Figure 6 shows the spectral dependence of the absorption coefficient measured at room temperature at $P=0$ and $P=2$ kbar. Two samples were used: a 2-mm-thick bulk sample and a self-supporting film 5 μm thick. The pressure-induced shift of the energy of the edge is independent of absorption coefficient α from 5 to 2×10^3 cm^{-1}. For As_2S_3 the shift was measured for bulk as well as thin film samples and was found to be independent of α. Since the shift of the edge is independent of absorption coefficient, although the exponential slope changes considerably (see Fig. 6), it is concluded that the shift is a change in E (horizontal shift) rather than a change in α (vertical shift).

The pressure-induced shift of the edge was measured at $T=200$ and 350 K as well as at room temperature. The energy at which $\alpha=5$ cm^{-1} is plotted as a function of P for the three temperatures in Fig. 7. The pressure-induced shift of the edge is independent of temperature over this range of temperatures ($\partial^2E_0/\partial P\partial T<5\times10^{-9}$ bar^{-1} K^{-1}).

Table IV summarizes the results of the pressure-induced shift of the absorption edge $(\partial E_0/\partial P)_T$ for the six materials measured here and for some other materials for comparison.

Most materials show a slight hysteresis on the first compression and none thereafter. Since the absorption edge shifts with annealing for many chalcogenide semiconductors, the pressure-induced shift of the absorption edge of $GeSe_2$ was measured before and after annealing at 250 °C for 1 h. This annealing caused the edge to shift to higher energy by about 0.2 eV. The pressure dependence of the edge changes from $(\partial E_0/\partial P)_T=-9\times10^{-6}$ eV bar^{-1} to -6×10^{-6} eV bar^{-1}.

There are two possible explanations for the change with annealing of the pressure dependence of the edge. It is probable that annealing increases the density and decreases the compressibility of amorphous solids. Then if the shift of the edge per unit strain was not changed by annealing, the ob-

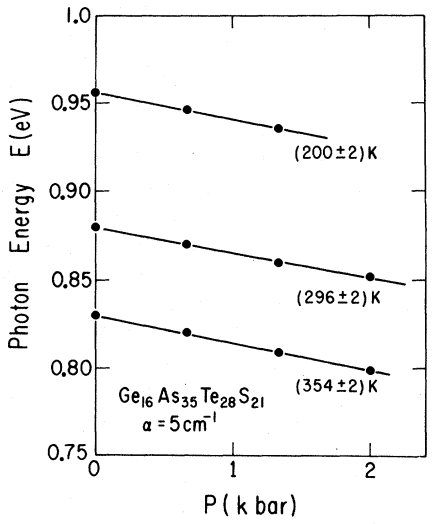

FIG. 7. The photon energy E at which the absorption coefficient $\alpha=5$ cm^{-1} versus P for three temperatures for alloy A. The pressure coefficient of the absorption edge is independent of temperature.

served $(\partial E_0/\partial P)_T$ would differ because of the change of compressibility. It is not likely, however, that annealing would cause a change in compressibility large enough to account for the 30% change in $(\partial E_0/\partial P)_T$. It can be seen from Table II, for example, that the compressibilities of fused and crystalline quartz differ by only about 3%.

Annealing of $GeSe_2$ probably causes a rearrangement of bonds. The few Ge-Ge bonds and Se-Se bonds formed during the sputtering of a film of $GeSe_2$ will probably rearrange during annealing to form the stronger Ge-Se bonds. Weak bonds may determine the properties of the absorption edge.[10] Therefore a reduction of the concentration of weak bonds should affect $(\partial E_0/\partial P)_T$.

We note that $(\partial E_0/\partial P)_T$ is negative for a-$GeSe_2$ but positive for a-Ge yet the edge shifts to higher energy with annealing for both materials. It has been suggested that the absorption edge of a-Ge shifts because stress is reduced by annealing.[27] The stress in a thin film is not hydrostatic. It is unlikely, however, in an isotropic material that the edge would shift to higher energy for hydrostatic pressure but to lower energy for uniaxial stress. If the shift of the edge with annealing is a result of stress relief, then the stress must be tensile for a-Ge but compressive for $GeSe_2$. Furthermore, the measured shifts with annealing are tenths of eV, which [judging from measured values of $(\partial E_0/\partial P)_T$] requires stresses of order 100 kbar. The stress in a-Ge has been measured to be ~2 kbar.[28] Therefore, the shift of the edge with annealing is probably not the result of decreasing stress in the film.

Our value of $(\partial E_0/\partial P)_T$ for alloy A is slightly larger than that reported by Fagen *et al.* [$-(1.2 \pm 0.1)\times 10^{-5}$ eV bar^{-1}]. We used a bulk sample of this material as did they. They used oil as the pressure medium and may not have corrected for the change in refractive index of the oil with pressure. Since we use He as the medium, no such correction is necessary.

Our value of $(\partial E_0/\partial P)_T$ for As_2Se_3 is considerably larger than that reported by Grant and Yoffe [$-(0.76 \pm 0.15)\times 10^{-5}$ eV bar^{-1}]. They measured the transmission of films on glass substrates. We consider it extremely important to use self-supporting films. Chalcogenide glasses have very large compressibilities—as much as five times that of silicate glasses—so that when the chalcogenide is on a silicate substrate the non-hydrostatic stresses are almost as large as the hydrostatic stresses. Our results for As_2Se_3 are only slightly smaller than those reported by Kolomiets and Raspopova[8] for the pressure-induced shift of the peak of the photoresponse curve (-1.7×10^{-5} eV bar^{-1}).

We can generalize from Table IV. $(\partial E_0/\partial P)_T$ is negative for chalcogenide semiconductors and positive for amorphous tetrahedral semiconductors. The latter is remarkable because the crystalline tetrahedral materials can have shifts of either sign. Furthermore, $(\partial E_0/\partial P)_T$ is of order 10^{-5} eV bar^{-1} for the group-IV deficient chalcogenides, but is an order of magnitude smaller for the tetrahedral materials. Since the compressibilities of the tetrahedral materials are an order of magnitude smaller than those of the chalcogenide-rich materials, the shift of E_0 per unit strain is of the same order for all materials. $V(\partial E_0/\partial V)_T$ is given in Table IV. We note, furthermore, that several molecular materials are known to behave in a manner similar to selenium when subjected to hydrostatic pressure. The results of Drickamer[29] on crystalline material as well as a-Se are reproduced in Fig. 8.

There are several excellent reviews[30,31] of the effects of pressure on the absorption edge of crystalline tetrahedral semiconductors. The pressure dependence of the absorption edge can be predicted if the band structure is calculated for different values of lattice constant. Connell and Paul[4] explored the question of whether the crystalline band structure of Ge, for example, could predict the pressure dependence of the absorption edge of amorphous Ge. They conclude that there is no correlation between $(\partial E_0/\partial P)_T$ of the crystal and that of the amorphous phase for the tetrahedral semiconductors.

Connell and Paul found that $(\partial E_\sigma/\partial P)_T$ [computed from $(\partial n/\partial P)_T$ and Eq. (8)] was greater than $(\partial E_0/\partial P)_T$ and both were positive for amorphous Si, Ge, GaAs, and GaP. This observation leads us back to the chemical-bond model. Consider Fig. 1(a). As the lattice constant decreases (increasing P) the bonding-antibonding energy separation increases $(\partial E_\sigma/\partial P > 0)$. Simultaneously the bonding and antibonding bands both broaden. Let the average of the broadening of valence and conduction band be $(\partial J/\partial P)_T > 0$. Then the band gap shifts as

$$\left(\frac{\partial E_0}{\partial P}\right)_T = \left(\frac{\partial E_\sigma}{\partial P}\right)_T - \left(\frac{\partial J}{\partial P}\right)_T \quad . \tag{21}$$

This is in qualitative agreement with the observations of Connell and Paul if the first term is larger than the second term on the right-hand side of Eq. (21).

Recall that the dielectric constant of Se is determined by Eq. (10). When the LL relation is the correct description of the dielectric constant the polarizability α_p can be described[3] by a one oscillator model

$$\alpha_p = A/E_\sigma^2 \tag{22}$$

with modified Penn-Phillips gap E_σ. In this case when pressure is applied, E_σ remains unchanged (α_p is independent of density). Closed-shell interactions, however, result in a broadening of bonding

and antibonding, as well as lone-pair bands. Therefore, in a molecular solid or a material with large bond-free solid angle we expect

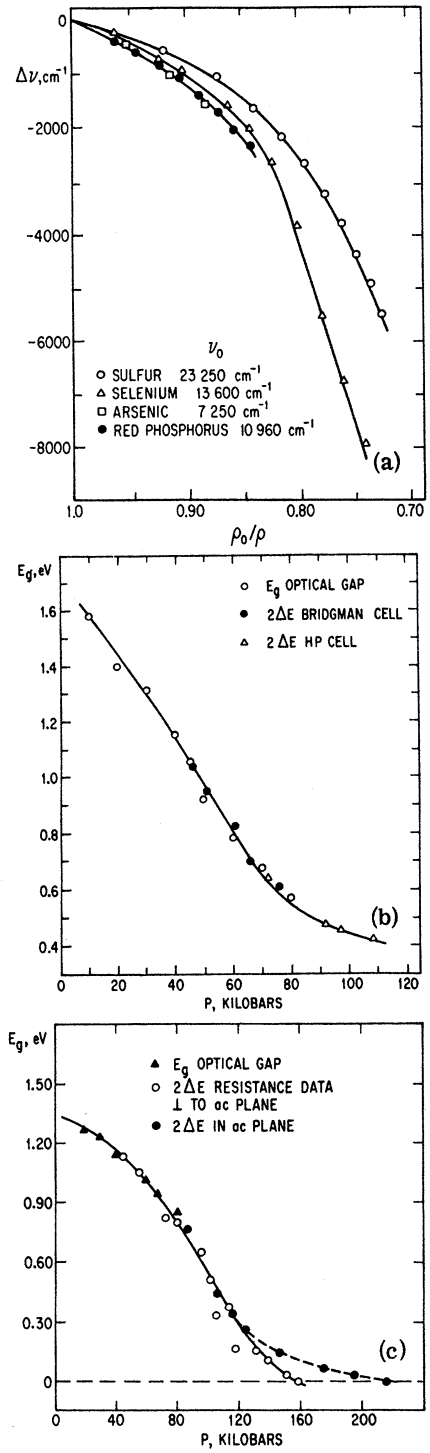

FIG. 8. (a) Shifts of absorption edges of some elements with density. (b) Energy gap versus pressure for selenium. (c) Energy gap versus pressure for iodine after Drickamer (Ref. 29).

$$\left(\frac{\partial E_0}{\partial P}\right)_T = -\left(\frac{\partial J}{\partial P}\right)_T . \tag{23}$$

This would always result in negative values of $(\partial E_0/\partial P)_T$. Furthermore, this mechanism can explain the observation of Drickamer[29] that many molecular solids have similar $(\partial E_0/\partial P)_T$. A few other mechanisms were examined to see if they can also explain the observed effects.

Dexter[32] showed that absorption below the fundamental absorption edge of a van der Waals solid (impurity absorption, for example) is enhanced by the local field. This, however, results in a shift of absorption coefficient (vertical shift) rather than the observed shift of E_0 (horizontal shift). Furthermore the effect can account for only 10% of the change in the logarithm of the absorption coefficient.

Dow and Redfield[33] (DR) propose that increased internal electric fields will broaden the absorption edge. Internal fields might be increased by pressure if Coulomb centers of opposite sign are forced closer together, for example. Using the theory of DR one predicts shifts of the edge arising from such mechanisms which are an order of magnitude smaller than the observed shifts.

Reitz[34] predicted that the absorption edge of Se and Te would shift to lower energy with increasing pressure because the bond angle increases. However, this effect is estimated to be $(\partial E_0/\partial P)_P \sim 5 \times 10^{-7}$ eV bar^{-1}, much smaller than the observed shifts.

Before concluding the discussion of the volume dependence of the absorption edge, the important measurements of Nunoshita and Arai[35] (NA) should be mentioned. They measured the activation energy of the dc conductivity, $\frac{1}{2}\Delta E$. They found for about 25 glasses in the Si-As-Te system

$$\Delta E = E_1 - \rho\delta , \tag{24}$$

where ρ is the density and E_1 and δ are constants. If a change in density arising from a difference in composition is equivalent to a change in density caused by the application of pressure, then $\delta = -V \times (\partial E_0/\partial V)_T$. For NA's materials, $\rho \sim 5$ and $\rho\delta \sim 3$ eV. Table IV gives $V(\partial E_0/\partial V)_T$ for several materials. For materials with large bond-free solid angle the values are about 2 eV. It appears that a change of density caused by a change in composition has an effect similar to that of a change in density caused by compression.

It is concluded that the simple chemical-bond model is a rather general explanation. The different sign of $(\partial E_0/\partial P)_T$ for low coordination number materials from that for tetrahedral materials arise from the difference in BFSA. As was the case for the refractive index, pressure measurements can separate the effects of closed-shell interactions

TABLE V. Separation of $(1/n)(\partial n/\partial T)_P$ into volume and electron-phonon terms. β is the volume expansion coefficient.

Material	β (10^{-5} K^{-1})	$\frac{1}{n}\left(\frac{\partial n}{\partial T}\right)_P$ (10^{-5} K^{-1})	$\frac{-\beta}{Kn}\left(\frac{\partial n}{\partial P}\right)_T$ (10^{-5} K^{-1})	$\frac{1}{n}\left(\frac{\partial n}{\partial T}\right)_V$ (10^{-5} K^{-1})
Diamond	0.3[a]	0.41[b]	0.095	0.32
c-Si	0.6[a]	3.9[c]	0.17	3.7
c-Ge	1.5[a]	6.9[c]	1.1	5.8
c-GaAs	1.5[a]	4.5[d]	0.78	3.7
a-SiO_2	0.15[e]	0.63[f]	−0.035	0.66
a-As_2S_3	7.8[g]	−0.94[h]	−5.5	4.6
a-alloy A	4.2[i]	3±4[h]	−4±1	7±5
a-Se	7[e]		−7.7	

[a]P. Aigrain and M. Balkanski, *Selected Constants Relative to Semiconductors* (Pergamon, Oxford, 1961).
[b]G. N. Ramachandran, Proc. Ind. Acad. Sci. A25, 266 (1947).
[c]M. Cardona, W. Paul, and H. Brooks, J. Phys. Chem. Solids 8, 204 (1959).
[d]M. Cardona, in *Proceedings of the International Conference on Semiconductor Physics* (Czechoslovak Academy of Science, Prague, 1961).
[e]*American Institute of Physics Handbook*, 2nd ed. (McGraw-Hill, New York, 1963).
[f]R. M. Waxler and C. E. Weir, J. Res. Natl. Bur. Stand. (U. S.) 69A, 325 (1965).
[g]Servo Corportation of America.
[h]Present work.
[i]Reference 5.

from those of chemical bonds for materials with large BFSA.

VII. TEMPERATURE DEPENDENCE OF REFRACTIVE INDEX

The chemical-band approach has enabled us to explain qualitatively the transitions in the pressure dependence of n and E_0. As can be seen from Table I, there is no similar transition in the values of $[\partial(nl)/\partial T]_P$ or $(\partial E_0/\partial T)_P$.

The temperature induced change of nl was measured between room temperature and 100 °C. The measurement of $[\partial(nl)/\partial T]_P$ for As_2S_3 is more precise than for the other materials because the technique of Schneider and Vedam was used, as described in Sec. II. Using Eq. (2) one can determine $(1/n)(\partial n/\partial T)_P$, which is listed in Table V. Because of the large expansion coefficient β for As_2S_3, the second term in Eq. (2) is large, so that the accuracy of the measurement depends on the accuracy of the value of β used. Malitson *et al.*[36] found differences among the values of $(\partial n/\partial T)_P$ for different samples of As_2S_3. For some samples the value was larger and for others smaller than the result reported here.

Any quantity $X(P, T)$ has two components in its temperature dependence:

$$\left(\frac{\partial X}{\partial T}\right)_P = \left(\frac{\partial X}{\partial T}\right)_V - \frac{\beta}{K}\left(\frac{\partial X}{\partial P}\right)_T . \tag{25}$$

Table V shows the values of the three terms in Eq. (25) for the refractive index of a few crystalline tetrahedral semiconductors and for amorphous SiO_2, As_2S_3, and alloy A. The volume term is large for As_2S_3 and alloy A because the expansion coefficients are large. Accurate determination of $(\partial n/\partial T)_V$ therefore requires accurate measurement of β and K. On the other hand, β is much smaller for the tetrahedral materials so that little error is introduced in evaluating $(1/n)(\partial n/\partial T)_P$ from Eq. (2). Furthermore the volume term is less than 25% of $(\partial n/\partial T)_V$ as can be seen from Table V. $(1/n)\times(\partial n/\partial T)_V$ is positive for all the materials. One might ascribe $(\partial n/\partial T)_V$ in Si and Ge to a change in the Penn-Phillips gap E_σ arising from electron-phonon interactions. From Eq. (12)

$$\frac{1}{\epsilon - 1}\left(\frac{\partial \epsilon}{\partial T}\right)_V = \frac{-2}{E_\sigma}\left(\frac{\partial E_\sigma}{\partial T}\right)_V . \tag{26}$$

In a material, like Se, which obeys the LL relation [Eq. (10)] with α_p independent of volume, $(1/n)(\partial n/\partial T)_V$ is related to a change in α_p [or E_σ in Eq. (22)] arising from electron-phonon interactions, if the magnitude of the local-field correction is independent of temperature. Wiser's calculation of local fields assumed zero temperature. If the localization of charge density is temperature dependent, the local-field correction will be temperature dependent, in which case Eq. (10) ceases to be a correct description of the dielectric constant. The situation is further complicated for materials like SiO_2 with intermediate average bond-free solid angle because the effects of closed-shell interactions and chemical bonds cannot be separated, and because there is no simple relation that can adequately describe the dielectric constant.

It appears from the results for As_2S_3 and Se in Table V that materials with large BFSA have large β. Since $(1/K)(\partial n/\partial P)_T$ is also large, the volume term will in general be a large fraction of the total temperature dependence for these materials. An accurate determination of $(\partial n/\partial T)_V$ then becomes difficult. More precise measurements of $(\partial n/\partial T)_P$, β, and K for solids with large BFSA must be carried out before we can accurately determine the electron-phonon interaction term contributing to $(\partial n/\partial T)_P$.

VIII. TEMPERATURE DEPENDENCE OF ABSORPTION EDGE

Many amorphous semiconductors have exponential absorption edges with slopes of order 40 meV at room temperature. For some of these the exponential slope is temperature dependent as observed for a-Se by Siemsen and Fenton.[37] Tauc *et al.*[38] measured the absorption coefficient of As_2S_3 and found that the exponential edge at $\alpha \gtrsim 1$ cm^{-1} shifts at a rate $\Delta E/\Delta T \approx -1.1\times10^{-3}$ eV K^{-1},

TABLE VI. Separation of $(\partial E_0/\partial T)_P$ into volume and electron-phonon terms.

Material	$\left(\frac{\partial E_0}{\partial T}\right)_P$ (10^{-4} eV K^{-1})	$\frac{-\beta}{K}\left(\frac{\partial E_0}{\partial P}\right)_T$ (10^{-4} eV K^{-1})	$\left(\frac{\partial E_0}{\partial T}\right)_V$ (10^{-4} eV K^{-1})
c-Si	-2.2[a]	0.08	-3.0
c-Ge	-3.7[b]	-0.56	-3.1
a-alloy A	-5[c]	0.8	-5.8
a-As_2S_3	-3[c]	0.8	-3.8

[a]J. R. Haynes, M. Lax, and W. F. Flood, J. Phys. Chem. Solids 8, 392 (1959).

[b]G. C. MacFarlane, T. P. McLean, J. E. Quarrington, and V. Roberts, Phys. Rev. 108, 1377 (1957).

[c]Present work.

which is three to four times larger than the shift measured at $\alpha \sim 3\times10^3$ cm^{-1} (Table I). It appears that the exponential slope decreases with temperature for As_2S_3 as well as Se. On the other hand, Fagen *et al.*[3] studied the absorption coefficient of alloy A between $\alpha \sim 1$ and $\alpha \sim 10^3$ cm^{-1} and found a rigid shift of the exponential edge with temperature.

Table VI shows the separation of $(\partial E_0/\partial T)_P$ into the volume term and the electron-phonon interaction term. The electron-phonon term is several times larger than the volume term for chalcogenide as well as tetrahedral materials. The volume change, as we have seen from pressure measurements, results in a rigid shift of the edge with no change in slope. Therefore any decrease of the exponential slope of the edge with increasing temperature, as well as the shift of the edge, is predominantly a result of electron-phonon interaction.

Mott[39] has suggested that the effect of increased temperature might be to reduce the separation R between chains or layers in the more molecular chalcogenide glasses, i.e., to act in the same direction as pressure. β is large and always positive so the *average* separation between molecular units increases with temperature. But $\langle R^2\rangle$ also increases with temperature. At some instant R may therefore be quite small. This would broaden the electronic levels resulting in a shift of the absorption edge to lower energy.

Tauc[40] has recently reviewed several models that attempt to account for exponential absorption edges. The theory of Dow and Redfield, for example, proposes that all exponential edges are caused by electric-field-enhanced ionization of the exciton. The electric fields can be caused by ionized impurities, phonons, or (as discussed by Fritzsche[41] for the case of amorphous semiconductors) by potential fluctuations. For larger average electric-fields the exponential slope of the edge is smaller—the edge is broader. At sufficiently high temperatures, phonon-induced electric fields will dominate, and the slope of the edge will be temperature dependent. Within the framework of this model one explains the fact that the slope of the edge is temperature dependent at room temperature for Se but not for alloy A by arguing that electric fields with origin different from phonons are so large in more complicated glasses that phonon fields will dominate only at higher temperatures. This explanation is somewhat unsatisfying. If the internal fields are much larger in alloy A than in Se or As_2S_3, the exponential slope should be smaller at low temperature. The slope is 0.045 eV for alloy A, ~0.04 eV for Se at 300 K,[37] and ~0.05 eV for As_2S_3 at 300 K.[38] The theory of Dow and Redfield, which is so appealing because of its generality, cannot explain the different temperature dependence of the exponential absorption edge for different amorphous semiconductors.

Other models of the exponential absorption edge will not be analyzed here. It should be emphasized, however, that although the temperature dependence of the exponential absorption edge is clearly a result of electron-phonon interaction, the mechanism of that interaction is not yet understood.

IX. CONCLUSIONS

The pressure dependence of the absorption edge and refractive index offers new evidence that there are important differences among amorphous semiconductors. I have previously pointed out some differences between tetrahedral and lone-pair semiconductors.[10] It is now realized that there are further differences between those lone-pair materials with large and small BFSA. We have seen that in Ge or Si bond compression dominates the pressure dependence of n and E_0. When bonds are compressed, n decreases because the bond strength (or E_σ) increases. E_0 increases but not as fast as E_σ because of band broadening. In materials with large BFSA, however, bonds are less affected by pressure than closed-shell interactions. In such materials local-field corrections make an important contribution to the refractive index and its volume dependence. Since pressure does not change bond lengths, the average energy separation between valence and conduction bands does not change. Therefore E_0 decreases with pressure because of band broadening.

The temperature dependence of the refractive index is also influenced by the average BFSA. For materials with small BFSA, most of $(\partial n/\partial T)_P$ arises from electron-phonon interaction, but for materials with large BFSA the expansion coefficient is large so the volume term is dominant.

The temperature dependence of the absorption edge, on the other hand, is predominantly a result of electron-phonon interactions both for materials

with large and small BFSA. Therefore, there are no strong trends in $(\partial E_0/\partial T)_P$ as a function of composition within the group of materials studied in this work.

I believe that the concept of bond-free solid angle will be helpful in understanding compositional trends other than those discussed here. For example, Emin[42] has proposed the existence of polarons in amorphous semiconductors. Materials with large BFSA have larger compressibilities and polaron formation is therefore more likely in these materials. Chalcogenide glasses can be used for acousto-optic modulation. They are favorable for this application because the stress coefficient of refractive index is large. This should be true of many materials with large BFSA because they have large compressibilities and the volume dependence of their refractive index is large because of large local-field corrections.

The BFSA concept is an extension of the chemical-bond approach that was employed previously[10] to predict trends in the properties of amorphous semiconductors as a function of composition. Since amorphous semiconductors cannot be easily doped, compositional variation must be used in order to change the electronic properties of these materials. It is hoped that in this way we may gain a better understanding of those properties.

ACKNOWLEDGMENTS

The author wishes to thank Energy Conversion Devices, Inc. for furnishing many samples of chalcogenide semiconductors and Servo Corporation of America for samples of As_2S_3. The help of M. Paesler in sample preparation is gratefully acknowledged. Most of all, the inspiration, guidance, and encouragement of my thesis advisor, Professor H. Fritzsche, are deeply appreciated.

---

*Submitted in partial fulfillment of the requirements for the Ph.D. degree at The University of Chicago.

†Work supported by Air Force Office of Scientific Research, Office of Aerospace Research, USAF, under Contract No. AF F44620-71-C-0025. We have also benefited from support of the Materials Research Laboratory by the National Science Foundation.

‡Fannie and John Hertz Foundation Fellow.

§Present address: Division of Engineering and Applied Physics, Harvard University, Cambridge, Mass. 02138.

[1]J. C. Phillips, Rev. Mod. Phys. **49**, 317 (1970).

[2]J. A. Van Vechten, Phys. Rev. **182**, 891 (1969).

[3]M. Kastner, Phys. Rev. B **6**, 2273 (1972).

[4]G. A. N. Connell and W. Paul, J. Non-Cryst. Solids **8**, 215 (1972).

[5]E. A. Fagen, S. H. Holmberg, R. W. Seguin, and J. C. Thompson, in *Proceedings of the Tenth International Conference on the Physics of Semiconductors, Cambridge, Mass., 1970* (U.S. AEC, Division of Tech. Information, Oak Ridge, Tenn., 1970), p. 672.

[6]W. C. Schneider and K. Vedam, J. Opt. Soc. Am. **60**, 800 (1970).

[7]A. J. Grant and A. D. Yoffe, Solid State Commun. 8, 1919 (1970).

[8]B. T. Kolomiets and E. M. Raspopova, Sov. Phys.-Semicond. **4**, 124 (1970).

[9]E. Mooser and W. B. Pearson, in *Progress in Semiconductors* (Heywood, London, 1960), Vol. 5, p. 104.

[10]M. Kastner, Phys. Rev. Lett. **28**, 355 (1972).

[11]J. N. Murrell, M. Randic, and D. R. Williams, Proc. R. Soc. A **284**, 566 (1965).

[12]R. S. Mulliken, J. Chem. Phys. **46**, 497 (1949).

[13]J. Treusch and R. Sandrock, Phys. Status Solidi **16**, 487 (1966).

[14]L. J. Bellamy, *The Infrared Spectra of Complex Molecules*, 2nd ed. (Methuen, London, 1958).

[15]N. Wiser, Phys. Rev. **129**, 62 (1963).

[16]S. Spinnner and R. M. Waxler, Appl. Opt. **5**, 1887 (1966).

[17]H. Mueller, Phys. Rev. **47**, 947 (1935).

[18]P. Y. Yu and M. Cardona, Phys. Status Solidi B **47**, 251 (1971).

[19]G. H. Meeten, Nature (Lond.) **218**, 761 (1968).

[20]D. A. Pinnow, IEEE J. Quantum Electron. **6**, 223 (1970).

[21]N. F. Mott and R. W. Gurney, *Electronic Processes in Ionic Crystals* (Oxford U. P., London, 1940).

[22]A. R. Hilton, C. E. Jones, and M. Brau, Phys. Chem. Glasses **7**, 105 (1966).

[23]N. A. Goryunova, *The Chemistry of Diamond-Like Semiconductors* (MIT Press, Cambridge, Mass., 1965).

[24]J. P. de Neufville, J. Non-Cryst. Solids **8**, 85 (1972).

[25]S. Sakka and J. D. Mackenzie, J. Non-Cryst. Solids **6**, 145 (1967).

[26]M. Nunoshita and H. Arai (unpublished).

[27]F. L. Galeener, Phys. Rev. Lett. **27**, 1716 (1971).

[28]A. E. Ennos, Appl. Opt. **5**, 51 (1966).

[29]H. G. Drickamer, in *Solid State Physics*, edited by F. Seitz and D. Turnbull (Academic, New York, 1965), Vol. 17.

[30]W. Paul, in *Colloque International Sur les Proprietes Physique des Solides Sous Pression* (Éditions du Centre de la Recherche Scientifique, Paris, 1970), p. 199.

[31]*Solids Under Pressure*, edited by W. Paul and D. M. Warschauer (McGraw-Hill, New York, 1963).

[32]D. L. Dexter, Phys. Rev. **101**, 45 (1955).

[33]J. D. Dow and D. Redfield, Phys. Rev. B **5**, 594 (1972); Phys. Rev. B **1**, 3358 (1970); Phys. Rev. Lett. **26**, 762 (1971).

[34]J. R. Reitz, Phys. Rev. **105**, 1233 (1957).

[35]M. Nunoshita and H. Arai (unpublished).

[36]I. H. Malitson, W. S. Rodney, and T. A. King, J. Opt. Soc. Am. **48**, 633 (1958).

[37]K. J. Siemsen and E. W. Fenton, Phys. Rev. **161**, 632 (1967).

[38]J. Tauc, A. Menth, and D. L. Wood, Phys. Rev. Lett. **25**, 749 (1970).

[39]N. F. Mott, Philos. Mag. **24**, 1 (1971).

[40]J. Tauc, in *Amorphous and Liquid Semiconductors*, edited by J. Tauc (Plenum, New York, to be published).

[41]H. Fritzsche, J. Non-Cryst. Solids **6**, 49 (1971); and in Ref. 40.

[42]D. Emin, Phys. Rev. Lett. 28, 813 (1972).